The Plant Journal (2004) **40**, 523–535 doi: 10.1111/j.1365-313X.2004.02230.x

Potassium carrier TRH1 is required for auxin transport in *Arabidopsis* roots

Francisco Vicente-Agullo[1], Stamatis Rigas[2], Guilhem Desbrosses[3,†], Liam Dolan[3], Polydefkis Hatzopoulos[2] and Alexander Grabov[1,*]

[1]*Department of Agricultural Sciences, Imperial College London, Wye Campus, Wye, Ashford, Kent TN25 5AH, UK,*
[2]*Laboratory of Molecular Biology, Agricultural University of Athens, Iera Odos 75, 118 55 Athens, Greece, and*
[3]*Department of Cell and Developmental Biology, John Innes Centre, Norwich Research Park, Colney, Norwich NR4 7UH, UK*

Received 23 April 2004; revised 9 August 2004; accepted 17 August 2004.
*For correspondence (fax +02 075 94 2640; e-mail a.grabov@imperial.ac.uk).
†Present address: Laboratoire des Symbioses Tropicales & Méditerranéennes, Université Montpellier II, Place E. Bataillon, 34095 Montpellier, Cedex 5, France.

Summary

Disruption of the TRH1 potassium transporter impairs root hair development in *Arabidopsis*, and also affects root gravitropic behaviour. Rescue of these morphological defects by exogenous auxin indicates a link between TRH1 activity and auxin transport. In agreement with this hypothesis, the rate of auxin translocation from shoots to roots and efflux of [^{3}H]IAA in isolated root segments were reduced in the *trh1* mutant, but efflux of radiolabelled auxin was accelerated in yeast cells transformed with the *TRH1* gene. In roots, Pro_{TRH1}:*GUS* expression was localized to the root cap cells which are known to be the sites of gravity perception and are central for the redistribution of auxin fluxes. Consistent with these findings, auxin-dependent *DR5:GUS* promoter-reporter construct was misexpressed in the *trh1* mutant indicating that partial block of auxin transport through the root cap is associated with upstream accumulation of the phytohormone in protoxylem cells. When [K^+] in the medium was reduced from 20 to 0.1 mM, wild type roots showed mild agravitropic phenotype and *DR5:GUS* misexpression in stelar cells. This pattern of response to low external [K^+] was also affected by *trh1* mutation. We conclude that the TRH1 carrier is an important part of auxin transport system in *Arabidopsis* roots.

Keywords: auxin, plant development, root, gravitropism, root hairs, K^+ transporters.

Introduction

The phytohormone auxin regulates a broad spectrum of cellular responses crucial for plant morphogenesis. In roots, auxin stimulates the development of secondary meristems (Thimann, 1936; Torrey, 1950), affects root cell elongation (Aberg, 1957; Cholodny, 1924; Lane, 1936), regulates root hair formation (Masucci and Schiefelbein, 1996; Meesters, 1936; Schiefelbein *et al.*, 1997) and is essential for gravitropic responses (Cholodny, 1924; Dolan, 1998; Estelle, 1996; Firn *et al.*, 2000; Went and Thimann, 1937).

Auxin is produced predominantly, but not exclusively, in the aerial parts of the plant (Bhalerao *et al.*, 2002; Müller *et al.*, 1998b) and redistributed within the plant body through a complex transport network. In roots, auxin is transported acropetally through the stellar tissues to the root cap columella where the direction of the phytohormone fluxes is reversed to basipetal and diverted to the cortical and epidermal cells (Baker, 2003; Dolan, 1998; Estelle, 1996; Marchant *et al.*, 1999). Gravistimulation of the columella cells is known to affect the lateral auxin distribution and basipetal fluxes rendering them asymmetrical. This asymmetry plays a key role in gravitropic responses, because an excess of auxin on the underside of the root curves the root down through the inhibition of cell growth (Estelle, 1996).

Acropetal long-distance auxin transport in roots is, probably, mediated by phloem cells that are characterized by high (approximately 1 μM) level of this phytohormone (Baker, 2003; Swarup *et al.*, 2001). After unloading from the phloem, further delivery of the phytohormone to the root apex is facilitated by the auxin carriers AUX1 and AtPIN1, which are localized asymmetrically in the protophloem cells of *Arabidopsis* roots. AUX1, a facilitator of auxin uptake, belongs to the LAX family of auxin permeases, while the

AtPIN auxin efflux carriers share some similarity with bacterial transporters (Swarup *et al.*, 2001).

The polarity of basipetal auxin transport in the apex is maintained by asymmetrical localization of AtPIN2 in epidermal (Müller *et al.*, 1998a) and lateral root cap (Friml, 2003) cells, where this auxin efflux carrier is preferentially localized to the upper anticlinal side of the cell (Müller *et al.*, 1998a). This pattern of AtPIN2 expression ensures directional basipetal auxin delivery to the elongation zone. The role of AtPIN2-mediated transport in gravitropic responses has been demonstrated in the *eir1-3* mutant, where, in contrast to the wild type (wt) plants, no auxin accumulation was detected in the underside of a gravistimulated root (Luschnig *et al.*, 1998). The function of other AtPIN efflux transporters is also important for gravitropism. One of these, AtPIN3, is crucial for the transmission of auxin signal from gravity-sensing cells such as starch sheath and columella (Friml *et al.*, 2002b), while AtPIN4 maintains auxin gradients in the root tips through the sink-mediated distribution (Friml *et al.*, 2002a).

To date, LAX and PIN carriers are the best characterized components of auxin transport system in *Arabidopsis* roots. Recent findings, however, indicate that these transporters, albeit important, do not exclusively facilitate auxin distribution. MDR-type ABC protein AtMDR1, for instance, mediates basipetal auxin transport in *Arabidopsis* hypocotyls. Impaired polar auxin transport in *Atmdr1* mutants causes epinasty of cotyledons and first leaves, which can be phenocopied by administration of the synthetic auxin 2,4-dichlorophenoxy acetic acid (2,4-D) (Noh *et al.*, 2001). Disruption of another ABC transporter *AtMRP5* causes a 100% increase in auxin levels in *Arabidopsis* roots and, consequently, reduction in root length. AtMRP5, probably, functions as a transporter of auxin conjugates (Gaedeke *et al.*, 2001).

Mutations in genes encoding some potassium transporters belonging to the *KT/KUP/HAK* multi-gene family (Fu and Luan, 1998; Kim *et al.*, 1998; Maser *et al.*, 2001; Quintero and Blatt, 1997; Rubio *et al.*, 2000) result in phenotypes resembling defects in auxin transport. One of these mutants, *t*iny *r*oot *h*air *1* (*trh1*), is impaired in root hair elongation (Rigas *et al.*, 2001), while *shy3-1* is characterized by the reduced length of hypocotyl cells (Elumalai *et al.*, 2002). Surprisingly, *trh1* and *shy3-1* phenotypes were not rescued by growing plants in the presence of high potassium concentrations and neither of these mutants displayed symptoms of potassium starvation (Desbrosses *et al.*, 2003; Elumalai *et al.*, 2002; Rigas *et al.*, 2001). These paradoxical observations imply an alternative morphogenic function for some KT/KUP/HAK proteins, which might be related to the transport of regulatory substances rather than to the bulk potassium accumulation. The fact that both elongation of hypocotyl cells and root hair growth are regulated by auxin (Collett *et al.*, 2000; Friml *et al.*, 2002b; Masucci and Schiefelbein, 1996; Meesters, 1936; Rahman *et al.*, 2002) prompted us to investigate the role of the TRH1 carrier in auxin transport. The results indicate that the TRH1 protein functions as a crucial component of the auxin transport system in *Arabidopsis* roots.

Results

Morphological defects in trh1 mutants are consistent with impaired auxin transport and can be rescued by treatment with auxin

Impaired development of root hairs is the most obvious morphological trait of the *trh1* mutant (Rigas *et al.*, 2001). Apart from this defect, the root development of the 2 DAG (days after germination) mutant was only marginally different from the wt *Arabidopsis* plants (Figure 1a,b,h,i). On 3–4 DAG, in contrast to the wt plants (Figure 1c), the direction of *trh1* root growth spontaneously deviated from vertical (Figure 1d). The agravitropic root behaviour is often observed in mutants defective in auxin transport (Marchant *et al.*, 1999; Müller *et al.*, 1998a) or signalling (Hobbie and Estelle, 1995; Leyser *et al.*, 1996; Nagpal *et al.*, 2000). The transition to agravitropic growth in the *trh1* mutant on 3 DAG coincides with the time at which dramatic changes in acropetal auxin transport occur in *Arabidopsis* seedlings (Bhalerao *et al.*, 2002).

To establish whether the agravitropic growth phenotype in *trh1* mutants (Figure 1d) is due to a defect in the *TRH1* function and not a mutation in another gene, we transformed the mutant plants with 7.1 kb genomic DNA spanning the *TRH1* gene including the 2000 bp upstream sequence (Rigas *et al.*, 2001). This genomic fragment fully complemented both the root hair (Rigas *et al.*, 2001) and agravitropic root growth phenotypes (Figure 1e). Similarly, these phenotypes were rescued by addition of exogenous auxins to the nutrient medium (Figure 1f,g,j,k,l). Addition of naphthalene-1-acetic acid (1-NAA) specifically rescued defect in root hair elongation in trichoblasts of the *trh1* mutant (Figure 1l). In line with previous data obtained in wt plants (Masucci and Schiefelbein, 1996), auxin did not cause ectopic root hair outgrowth (Figure 1l).

Root growth pattern is often quantified as an angle between a base-to-tip chord and the vector of gravity (Fujita and Syono, 1996; Marchant *et al.*, 1999). This approach does not entirely account for the history of root development before the measurements are made and, thus, has a limited applicability for the quantitative description of the root growth pattern. In order to improve the accuracy and sensitivity of the morphometric analysis we introduced a parameter designated as the Vertical Growth Index (VGI), which is defined as the ratio between a vertical projection of the base-to-tip chord and the root length (see Figure 2a and Experimental procedures).

We used the VGI for quantitative analysis of root morphology in *trh1* and wt plants. This analysis indicates that

gravitropic behaviour in the 2 DAG *trh1* plants compared with the wt was impaired only by 8% (Figure 2b). After further 2 days of growth, the VGI of the 4 DAG *trh1* plants dropped dramatically from 0.87 ± 0.02 to 0.54 ± 0.05, while the gravitropic behaviour of the wt roots was only marginally reduced by 0.05 unit. These results demonstrate that the difference between the *trh1* and the wt plants in their ability to maintain gravitropic growth is more pronounced in the older 4 DAG seedlings. Therefore, for further morphological, physiological and molecular analysis we used 4–6 DAG plants.

The 4 DAG *trh1* plants transformed with the *TRH1* gene were characterized by VGI = 0.95 ± 0.01 that matched nearly exactly the VGI of wt plants (0.96 ± 0.01, Figure 2b). These quantitative data unequivocally demonstrate that the

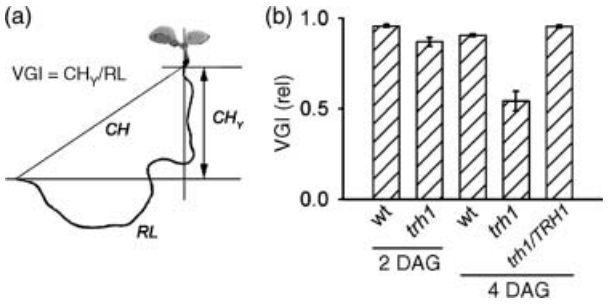

Figure 2. Definition of the Vertical Growth Index (VGI) and morphometric analysis of *Arabidopsis* roots.
(a) VGI is defined as a ratio between the vertical projection CH_Y of the base-to-tip chord CH and the root length RL.
(b) VGI of roots of wild type (wt) plants, *trh1* mutants and *trh1* plants transformed with genomic DNA spanning the *TRH1* gene (*trh1/TRH1*). VGI of the trh1 plants drops dramatically on 4 DAG. VGI of the *trh1/TRH1* plants is equal to VGI of wt plants. Data shown are mean ± SE, $n = 25$ or 30 plants.

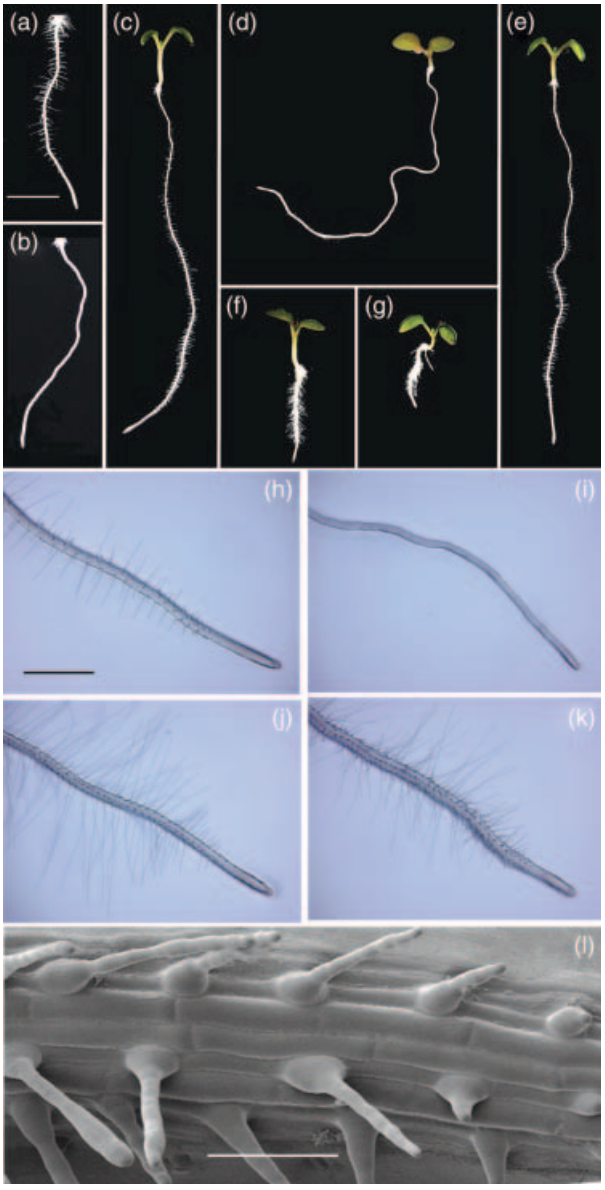

defect in gravitropism in the *trh1* mutants is a result of mutation in the *TRH1* gene.

To address in more detail the link between the morphogenic activity of the TRH1 protein and auxin-dependent processes we grew the plants on media supplemented with different concentrations of 2,4-D, 1-NAA, indole acetic acid (IAA) and a weak auxin 2-NAA. All these substances inhibited root elongation in both *trh1* and wt plants, but were effective in different ranges of concentration (Figure 3a–d). 2,4-D was the strongest inhibitor of wt root elongation characterized by the half-inhibition concentration $IC_{50} = 15.2 \pm 1.6$ nM (Figure 3a). While 1-NAA and IAA were twofold less active ($IC_{50} = 31.7 \pm 1.1$ and 36.3 ± 1.0 nM; Figure 3b,c respectively), inhibitory activity of 2-NAA ($IC_{50} = 443 \pm 6$ nM) was 30-fold weaker than that of 2,4-D (Figure 3d).

Figure 1. Morphological phenotypes of *trh1* roots are dependent on plant age and rescued by transformation with *TRH1* genomic DNA or by exogenous auxin.
(a) Two days after germination (DAG) wild type (wt) root. Scale bar = 2 mm. The same magnification is used in (b–f).
(b) *trh1* mutant roots (2 DAG) with a severe defect in root hair development, but less affected gravitropic behaviour.
(c) Gravitropic pattern of root development in 4 DAG wt plants.
(d) Impaired gravitropic growth in 4 DAG *trh1* mutants.
(e) Gravitropism and root hair growth rescued in the *trh1* mutants transformed with DNA spanning the *TRH1* gene including the 2000 bp upstream sequence.
(f) Wt plants (6 DAG) grown in the presence of 60 nM IAA.
(g) Addition of 60 nm IAA rescues gravitropism and root hair growth in 6 DAG *trh1* mutants.
(h) Root hairs of the 6 DAG wt root. Scale bar = 1 mm. The same magnification is used in (i–k).
(i) Root hairs fail to elongate in the *trh1* mutant (6 DAG seedling).
(j and k) Root hair elongation stimulated by NAA (80 nM) in wt (j) and *trh1* (k) 6 DAG seedlings.
(l) NAA (80 nM) specifically rescues root hair elongation in the *trh1* mutant but does not induce ectopic root hair growth. Scale bar = 0.1 mm.

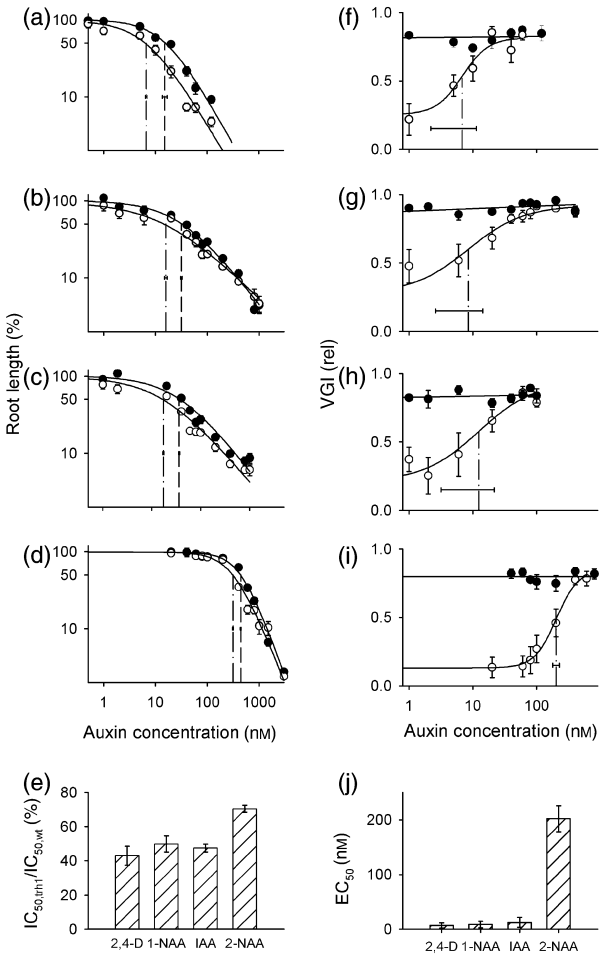

Figure 3. Effect of auxins on root elongation and Vertical Growth Index (VGI) in wild type (wt) plants and *trh1* mutants.
(a–e) Auxin-dependent inhibition of root elongation is exacerbated in the *trh1* mutant. Root length was measured in 6 DAG wt (●) and *trh1* (○) plants grown in the presence of 2,4-D (a), 1-NAA (b), IAA (c) or weak auxin 2-NAA (d). Half-inhibition concentrations (IC_{50}) are indicated by the drop lines (wt – dashed, and *trh1* – dot-dashed). Horizontal bars are SE of IC_{50}. Each point in (a–c) represents mean ± SE of $n = 20$–25 plants. Relative changes in auxin sensitivity caused by the *trh1* mutation are shown in (e) as $IC_{50,trh1}/IC_{50,wt}$ ratio. (f–j) Exogenous auxins rescue gravitropism in the *trh1* mutants. VGI was measured in 6 DAG wt (●) and *trh1* (○) plants grown in the presence of 2,4-D (f), 1-NAA (g), IAA (h) or weak auxin 2-NAA (i). Each point in (f–i) represents mean ± SE of $n = 20$–25 plants. Effective mid-point concentrations (EC_{50}) at which 50% of gravitropic response in *trh1* is rescued are indicated by drop lines in (f–i) and are shown in the linear scale as mean ± SE in (j). Horizontal bars in (f–i) represent SE of EC_{50}.

Qualitatively, auxins have a similar effect on the elongation of *trh1* roots. 2,4-D ($IC_{50} = 6.6 \pm 0.24$ nM, Figure 3a) was more active than 1-NAA and IAA ($IC_{50} = 15.8 \pm 0.9$ nM and 17.2 ± 0.5 nM, Figure 3b,c respectively). Again, the weakest inhibitor of *trh1* root elongation was 2-NAA ($IC_{50} = 312 \pm 5$ nM), which was 50-fold less active than 2,4-D (Figure 3d). In comparison with wt plants, inhibition of root elongation in *trh1* mutants was observed at lower auxin concentrations (Figure 3a-d). The shift in auxin sensitivity caused by the *trh1* mutation was quantified with the use of normalized half-inhibition concentrations (Simmons *et al.*, 1995) calculated as a ratio between IC_{50} values of the *trh1* and wt roots ($IC_{50,trh1}/IC_{50,wt}$, Figure 3e). This analysis indicated that the *trh1* mutants are approximately twofold more sensitive to all active auxins (2,4-D, 1-NAA and IAA) than the wt plants ($IC_{50,trh1}/IC_{50,wt} = 43 \pm 5$, $49 \pm 5\%$ and $48 \pm 2\%$ respectively). The difference in sensitivity to 2-NAA was less significant ($IC_{50,trh1}/IC_{50,wt} = 70 \pm 2\%$). The observed hypersensitivity of the *trh1* roots to exogenous auxin might indicate that the mutation affects an ability of root cells to expel excess of auxin (Chen *et al.*, 1998; Luschnig *et al.*, 1998; Müller *et al.*, 1998a).

None of the auxins had an effect on the gravitropic behaviour of the wt roots (Figure 3f-i). VGI of the *trh1*, in contrast, was increased with concentrations of active auxins. When the growth media was supplemented with approximately 80 nM of 2,4-D, 1-NAA or IAA, the VGI of the *trh1* mutant approached the VGI of the wt plants indicating complete rescue of the gravitropic phenotype (Figure 3f–h). 2-NAA caused similar changes in the VGI of the *trh1* plants, but was effective at much higher concentrations (Figure 3i). Calculation of the effective mid-point concentrations (EC_{50}; Figure 3f–j) showed that 2,4-D ($EC_{50} = 6.8 \pm 4.6$), 1-NAA ($EC_{50} = 8.5 \pm 5.9$ nM) and IAA ($EC_{50} = 12.4 \pm 9.2$ nM) had a similar effect on the restoration of gravitropic growth in *trh1* plants, while 2-NAA was approximately 20–30-fold less efficient ($EC_{50} = 202 \pm 24$ nM).

The abnormal root gravitropic behaviour can be caused either by defects in establishing gravitropic set-point angle (GSA) (Digby and Firn, 1995) or by impaired gravity perception, signal transduction and differential growth. To find out what aspect of gravitropic behaviour is affected by the *trh1* mutation, the gravitropic response in the mutant and wt roots was assayed in short-term experiments as an ability to re-direct root growth after rotation of the plate with seedlings by 90° (Marchant *et al.*, 1999). To eliminate a contribution of phototropic reactions, these experiments were performed in the dark (Marchant *et al.*, 1999). The measurements indicated that after plate rotation the axial polarity in wt plants was re-orientated by $30.5 \pm 2.4°$ (Figure 4). Reduction of this response by 30% in the *trh1* mutant (Figure 4) indicates that some fast components of gravitropic response are impaired. We cannot rule out, however, additional effects of the *trh1* mutation on GSA. Supplementation of growth media with 60 nM 1-NAA stimulated the rotation of root growth axes by 55% in wt and by 180% in *trh1* mutants. In 1-NAA gravitropic response of the *trh1* mutant was stronger than in wt ($57.9 \pm 2.7°$ and $47.4 \pm 2.2°$ respectively). This latter phenomenon does, probably, have the same origin as hypersensitivity of root elongation to external auxin (Figure 3) indicating that *trh1* accumulates more exogenous auxin than wt plants.

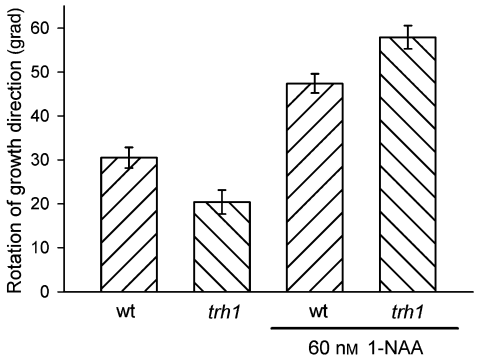

Figure 4. Reorientation of root growth direction in wild type (wt) plants and *trh1* mutants after 90° rotation of the plates with seedlings. Addition of 60 nM 1-NAA restores gravitropic response in *trh1* mutants.
Each bar is mean ± SE of $n = 20$ seedlings.

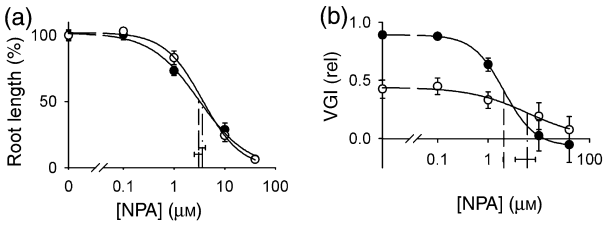

Figure 5. N-1-naphthylphthalamic acid (NPA) inhibits root elongation and gravitropic behaviour in wild type (wt) plants and *trh1* mutants.
(a) NPA-dependent inhibition of root elongation in wt plants (●) and *trh1* mutants (○). Half-inhibition concentrations (IC_{50}) are indicated by the drop lines (wt – dashed, and *trh1* – dot-dashed). Horizontal error bars are SE of IC_{50}. Each point is mean ± SE of $n = 25$ seedlings.
(b) Gravitropic behaviour of the *trh1* roots (○) is less sensitive to NPA than that of the wt roots (●). Half-inhibition concentrations (IC_{50}) are indicated by the drop lines (wt – dashed, and *trh1* – dot-dashed). Horizontal bars are SE of IC_{50}. Each point is mean ± SE of $n = 25$ seedlings.

The observed parallel between defects in root hair development and agravitropic phenotype was earlier found in some auxin-signalling AUX/IAA mutants (Fukaki *et al.*, 2002; Leyser *et al.*, 1996; Nagpal *et al.*, 2000). Unlike agravitropic AUX/IAA auxin-resistant mutants, roots of *trh1* plants were more sensitive to exogenous auxins than roots of wt plants. Hypersensitivity of *trh1* root elongation to exogenous 1-NAA and IAA (Figure 3b,c,e) is consistent with the physiology of the mutants defective in auxin efflux (Müller *et al.*, 1998a). However, in contrast to both auxin efflux and influx mutants (Marchant *et al.*, 1999; Müller *et al.*, 1998a), *trh1* displayed increased sensitivity to 2,4-D (Figure 3a,e). This finding indicates that if TRH1 is involved in auxin transport the underlying mechanisms are, probably, different from those of LAX and PIN transporters. TRH1 may facilitate auxin transport directly or, alternatively, indirectly by modulation of auxin fluxes through some other specific transporters. The data shown in Figure 3 are in line with both these theories. Alternatively, TRH1 may be crucial for some auxin-signalling events different from those observed in *axr* mutants.

trh1 roots are less sensitive to the inhibitor of auxin efflux transport, N-1-naphthylphthalamic acid (NPA)

The role of the TRH1 carrier as a facilitator of the efflux of auxin was implied by experiments in which *trh1* and wt roots were grown in the presence of the phytotropin NPA, an inhibitor of carrier-mediated auxin efflux (Delbarre *et al.*, 1996; Morgan and Söding, 1958; Sussman and Goldsmith, 1981) and root gravity response (Katekar and Geissler, 1980; Rashotte *et al.*, 2000). NPA also inhibits root elongation (Katekar and Geissler, 1980), probably due to the weak auxin activity of this phytotropin (Keitt and Baker, 1966).

In our experiments NPA treatment caused inhibition of root elongation to a similar extent in both wt and *trh1* plants (Figure 5a). Consistent with the weak auxin mode of action, IC_{50} values of the phytotropin were approximately 200-fold higher than those of 2,4-D. Similar inhibition of wt and *trh1* root growth indicates that TRH1 is not involved in NPA transport.

N-1-naphthylphthalamic acid treatment also inhibited the gravitropic behaviour in both wt and mutant roots. This effect was less pronounced in the *trh1* roots, which were threefold less sensitive to the phytotropin as assessed through the calculation of half-inhibition concentrations ($IC_{50} = 2.0 \pm 0.01$ and 6.0 ± 2.6 μM for wt and *trh1* respectively, Figure 5b). The low sensitivity of the mutant to the phytotropin suggests that an efflux transport activity targeted by NPA in the wt plants is disrupted in the *trh1* mutants. However, it is unlikely that NPA interacted with TRH1 directly as this phytotropin did not affect TRH1-dependent auxin efflux in transgenic yeast (not shown).

TRH1 accelerates auxin efflux in root segments and in transgenic yeasts

To test further the involvement of TRH1 in facilitation of auxin efflux we measured the net rate of [^{3}H]IAA accumulation in the *trh1* mutant roots using wt plants as a control. After 2 h incubation in [^{3}H]IAA, the mutant roots accumulated 45% more radioactivity than the wt control (Table 1). This higher rate of net label accumulation in the *trh1* roots suggests that the mutant exhibits either an increase in unidirectional influx of auxin or a reduction in efflux of this phytohormone. To distinguish between these two alternatives we measured the rate of the label efflux from the roots pre-loaded with [^{3}H]IAA. No statistically significant [^{3}H]IAA efflux was detected in the *trh1* plants. Wt roots, however, lost approximately 22% of accumulated label within 3 h of the wash (Table 1). The results of these two sets of experiments (Table 1) suggest that TRH1 activity assists auxin efflux in *Arabidopsis* roots.

Table 1 Accumulation, retention and translocation of [^{3}H]IAA in the wild type (wt) and *trh1* root segments, mean ± SE (*n*)

	Accumulated after 2 h incubation in 74 nM [^{3}H]IAA (fmol mg^{-1} FW)	Retained after 3 h wash of roots pre-floaded with [^{3}H]IAA (%)	Rate of translocation from base to the tip (fmol h^{-1} mg^{-1} FW)
Wt	486 ± 38 (4)	78 ± 8 (4)	25.5 ± 6.4 (6)
trh1	705 ± 22 (4)	101 ± 3 (4)	7.6 ± 2.7 (6)

n, number of replicates (10 root segments per replicate).

To verify the results of *in planta* experiments we measured auxin fluxes in yeast cells transformed with the *TRH1* gene. After 15 min incubation, cells expressing the TRH1 carrier accumulated 32% less [^{3}H]IAA than the control line transformed with the empty vector (Figure 6, Inset). Furthermore, the release of label by the *TRH1* transgenic yeast preloaded with [^{3}H]IAA was approximately 2.2-fold faster ($t_{1/2} = 3.3$ min) than by the control cells ($t_{1/2} = 7.4$ min; Figure 6). These data show that TRH1 activity accelerates the efflux of auxin from the cell into the medium.

Local application of [^{3}H]IAA to the basal end of the root segment and subsequent analysis of label translocation revealed the role of the TRH1 carrier in long-distance auxin transport. Compared with the wt plants, the rate of label translocation towards the tip in the *trh1* roots was reduced by 70% (Table 1). This reduction in auxin supply to the root apex is, probably, a primary cause of aberrations in gravitropic responses and root hair development in the *trh1* mutant.

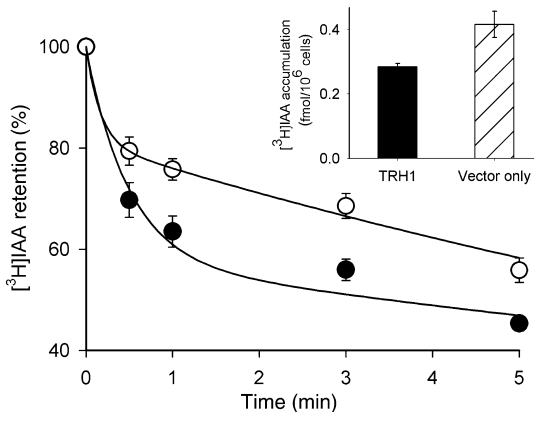

Figure 6. Retention and accumulation of [^{3}H]IAA in *Saccharomyces cerevisiae* strain M398 transformed with either empty pVT100U vector or vector containing the *TRH1* gene.
Cells pre-loaded with [^{3}H]IAA auxin were washed in auxin-free solution. Yeast expressing the *TRH1* gene (●) release label faster than yeast transformed with the empty vector (○). Each point is mean ± SE, $n = 12$ replicates (1.5×10^6 cells per replicate).
(Inset) Yeast expressing the *TRH1* gene (solid bar) accumulate less label than the cells transformed with empty vector (hatched bar). Cells were incubated for 15 min in the medium containing [^{3}H]IAA. Data shown are mean ± SE, $n = 4$ replicates (1.5×10^6 cells per replicate).

TRH1 expression pattern is consistent with its function in auxin transport system

TRH1 expression was studied in wt *Arabidopsis* plants transformed with the *GUS* reporter under the control of 2000 bp TRH1 promoter (*Pro$_{TRH1}$:GUS*, Figure 7a,b). This promoter is sufficient to drive the expression of the *TRH1* gene for complementation of the *trh1* phenotype (Figures 1e and 2b). Surprisingly, histochemical analysis did not reveal GUS staining in the root epidermal cells. Instead, the construct expression was localized mainly to the columella and the lateral root cap (Figure 7a) where the highest level of GUS activity was detected in tiers 2 and 3 of the columella (Figure 7b). These findings suggest that TRH1 may have a non-cell autonomous effect on the development of root hairs and gravity-dependent cell elongation.

The results of reporter-promoter expression experiments were verified by quantitative RT-PCR (qRT-PCR). The *TRH1* transcripts were analysed in the root apices and decapitated root segments (Figure 7c,inset). The apical root segments were 0.6 mm long and contained the entire root cap. The 10 mm long decapitated segments spanned the zone of root hair development from differentiation to maturation. The amount of *TRH1* transcripts detected in root segments by qRT-PCR and normalized per total RNA was 23-fold higher in the root tip than in the root hair development zone (Figure 7c). These data are compatible with the results of the promoter-reporter experiments (Figure 7a,b) indicating that *TRH1* is preferentially expressed in the root cap. qRT-PCR data also show that in other cell types there is some weak (approximately 4% of total) *TRH1* expression, which is not detectable histochemically.

Our results are qualitatively similar to recently published RT-PCR data (Ahn *et al.*, 2004) which demonstrate that *TRH1* (*AtKT3*/*AtKUP4*) is strongly expressed in the 1 mm long root tip segment containing the root cap. *TRH1* transcripts were also detected in RNA isolated from mature root hairs. However, only the end point products generated in 40 amplification cycles were shown (Ahn *et al.*, 2004). Because of saturation of the amplification curve at 40 cycles (Figure 7d) the literature data (Ahn *et al.*, 2004) do not indicate the relative strength of *TRH1* expression in different parts of the roots and cannot be quantitatively compared with our results.

Localized expression of the *TRH1* gene in root cap cells, which is crucial for gravity perception and redistribution of auxin (Blancaflor *et al.*, 1998; MacCleery and Kiss, 1999; Ottenschlager *et al.*, 2003), is consistent with its role in auxin transport. Other genes encoding auxin transport proteins such as *AUX1*, *AtPIN2*, *AtPIN3* and *AtPIN4* are also expressed in different subsets of columella and lateral root cap cells (Friml, 2003; Friml *et al.*, 2002a,b; Müller *et al.*, 1998a; Swarup

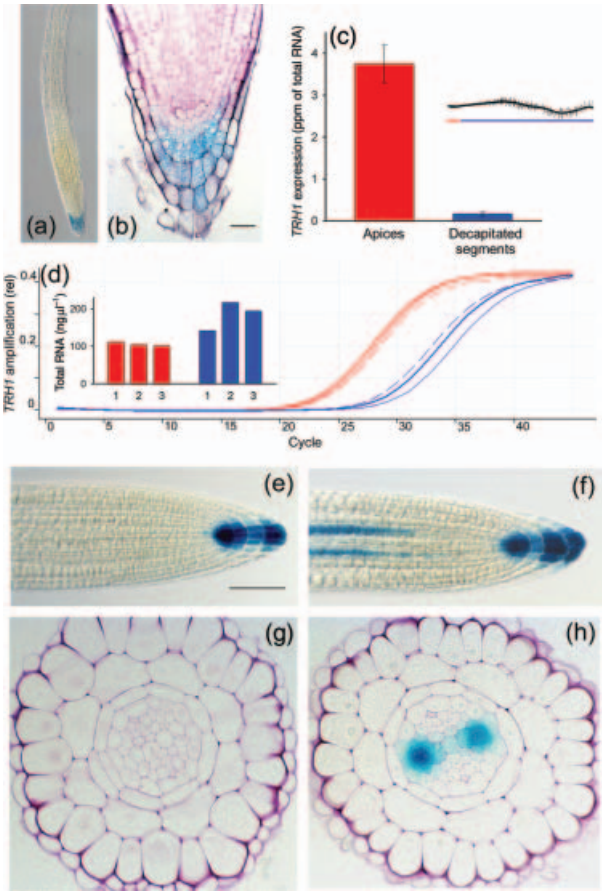

Figure 7. Expression of Pro_{TRH1}:*GUS* and *DR5:GUS* constructs.
(a) Five days after germination (DAG) root expressing Pro_{TRH1}:*GUS* construct. GUS activity is localized to columella and lateral root cap.
(b) Longitudinal section of the root tip expressing Pro_{TRH1}:*GUS*. In the root cap the highest level of *TRH1* expression was observed in the second and third tiers of the columella. Preparation is counterstained with ruthenium red. Scale bar represents 20 μm for (b) and 140 μm for (a).
(c and d) Quantitative RT-PCR (qRT-PCR) analysis of the TRH1 transcripts. *TRH1* expression in 0.6 mm root apices and 10 mm decapitated root segments (c). Each bar represents mean ± SE of $n = 3$ replicates (35–48 roots in a replicate). Roots were dissected as shown in (c, inset). The data in (c) were derived from SYBR Green amplification plots (d) obtained for transcripts from apices (red) and decapitated root segments (blue). The curves (dashed, solid thin and solid) were obtained in experiments 1,2 and 3 respectively. Total RNA in each sample is shown in (d, inset), apices – red, decapitated segments – blue.
(e and g) Expression of *DR5:GUS* in wild type (wt) roots grown on Murashige–Skoog solidified media. Highest GUS activity was detected in the quiescent centre, columella initials and mature columella root cap but not in the stele. (e) *DR5:GUS* expression in the tip of the 4 DAG wt root. (g) Transverse section of the GUS-stained root counterstained with ruthenium red. Scale bar shown in (e) represents 75 μm for (e) and 30 μm for (g).
(f and h) *trh1* plants grown on Murashige–Skoog solidified media display additional site of *DR5:GUS* expression in the protoxylem cell files. (f) *DR5:GUS* expression in the tip of the 4 DAG *trh1* roots. (h) Transverse section of GUS-stained root counterstained with ruthenium red. Scale bar shown in (e) represents 75 μm for (f) and 30 μm for (h).

et al., 2001). Given the association of the TRH1 carrier with the auxin transport function, root cap localization can also explain the role this protein plays in root hair development, as auxin is delivered to the epidermis through the lateral root cap (Friml, 2003). Similar to *trh1*, the *aux1* mutation affects not only root gravitropism (Swarup *et al.*, 2001) but also causes defects in root hair elongation (Rahman *et al.*, 2002). The defects in gravitropism are often accompanied by impaired root hair development in the AUX/IAA auxin-signalling mutants. In contrast to *trh1*, the auxin-signalling mutants display a larger array of phenotypes and, in most cases, are also impaired in shoot development (Fukaki *et al.*, 2002; Leyser *et al.*, 1996; Nagpal *et al.*, 2000).

Misexpression of DR5:GUS construct indicates distortion of auxin profile in the trh1 roots

The role of the TRH1 carrier in the auxin transport was examined by analysis of the expression of *DR5:GUS* (Ulmasov *et al.*, 1997) in the wt and the *trh1* background phenotype. β-glucuronidase in the *DR5:GUS* construct is controlled by a synthetic auxin-responsive element and, when assayed histochemically, provides an indication of auxin activity in the tissue (Ulmasov *et al.*, 1997). Wt plants displayed the highest GUS activity in the quiescent centre, columella initials and mature columella root cap (Figure 7e) (Sabatini *et al.*, 1999). The GUS staining pattern in the mutant (Figure 7f) was qualitatively different from the wt plants. As shown in Figure 7(f–h) disruption of the TRH1 transporter caused additional accumulation of GUS activity in the protoxylem cell files of the stele in the distal elongation zone (DEZ) (Mullen *et al.*, 1998). This pattern of expression was never observed in the wt plants of the same age and grown in similar conditions (Figure 7e,g). The elevated accumulation of auxin in the central cylinder is, probably, due to the disruption of the TRH1-dependent auxin transport downstream in the root cap cells. We suggest that this disruption of transport in the root cap affects the supply of auxin to cortical and epidermal cells in the DEZ and causes such phenotypical alterations in the *trh1* plants as impaired root hair development (Rigas *et al.*, 2001) and agravitropic root growth (Figure 1d). The suggested auxin deprivation of the cortical and epidermal cells is consistent with the decreased rate of net auxin supply to the root tip observed in the *trh1* mutant (Table 1).

trh1 mutation affects root response to changes in external K^+

To reconcile potassium transport function of the TRH1 with its role in auxin translocation in *Arabidopsis* roots we studied the effect of external potassium on root development and *DR5:GUS* expression in the *trh1* and wt plants. After 2 DAG growth on Murashige–Skoog phytagel solidified media, the plants expressing *DR5:GUS* construct were transferred to new agarose plates containing K^+-free assay media supplemented either with 0.1 or 20 mM KNO_3. After

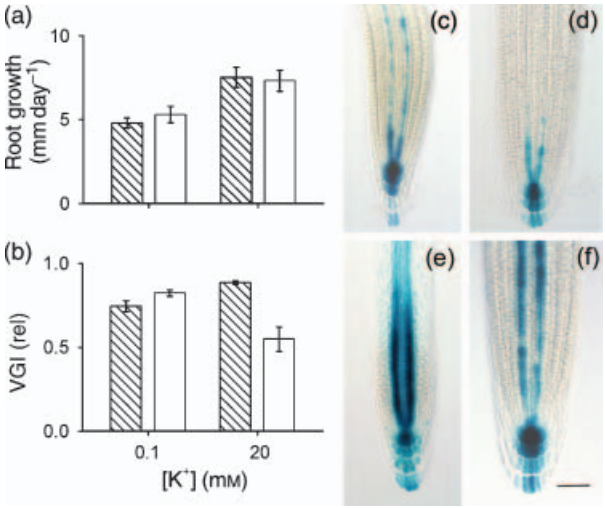

Figure 8. Root growth and DR5:GUS expression pattern in 6 DAG seedlings grown for 3 days on media containing different concentrations of K^+. During first 2 DAG plants were grown on standard phytagel-solidified Murashige–Skoog media and then the seedlings were transferred to agarose-solidified assay media (see Experimental procedures) containing 0.1 or 20 mM K^+.
(a) The rate of root elongation is lower in 0.1 mM K^+ in both wt and *trh1* seedlings.
(b) Deviation from vertical growth quantified with use of Vertical Growth Index (VGI) was differently affected by external K^+ in wt and *trh1* seedlings. Reduction in external K^+ triggered agravitropic behaviour in wt roots, while partially restoring gravitropic growth in the *trh1* roots.
(c and d) *DR5:GUS* expression in wt background phenotype when grown in 20 mM (d) or 0.1 mM (c) external K^+. At both K^+ concentrations DR5:GUS was expressed in QC, mature columella cell, stele initials and some adjacent young stellar cells. Low K^+ caused accumulation of GUS activity in central cylinder cell files in the distal elongation zone.
(e and f) *DR5:GUS* expression in *trh1* background phenotype when grown in 0.1 mM (e) or 20 mM (f) external [K^+]. Transfer of the *trh1* plants to 0.1 mM K^+ triggered changes in *DR5:GUS* expression pattern and some alterations in root morphology. Scale bar is 50 μm. The same magnification was in (c–e).

additional 3 days of growth on the assay media we analysed root morphology and expression pattern of *DR5:GUS* in the mutant and wt plants. In 20 mM K^+ (control) growth rate of the *trh1* roots (7.3 ± 0.6 mm day^{-1}) was similar to wt (7.5 ± 0.6 mm day^{-1}). Growth rate of both *trh1* and wt roots was equally inhibited by the reduction in external K^+ (4.8 ± 0.3 and 5.3 ± 0.5 mm day^{-1} respectively, Figure 8a).

After 3 day growth in control media containing 20 mM K^+, the gravitropic behaviour of the *trh1* and wt roots (Figure 8b) was very similar to those observed in standard Murashige–Skoog media (Figures 1c and 2b). Under these experimental conditions VGI of the 5 DAG *trh1* and wt roots were 0.55 ± 0.07 and 0.89 ± 0.01 respectively (Figure 8b). In low external K^+ roots of both plant types were thinner (Figure 8c,e). Interestingly, reduction in external [K^+] caused an increase of VGI in *trh1* roots (0.83 ± 0.02, Figure 8b), but affected negatively the gravitropic growth pattern of wt roots (VGI $= 0.74 \pm 0.03$, Figure 8b). Root hair development in both wt and mutant plants is not affected by low external potassium (Desbrosses *et al.*, 2003).

In roots grown on agarose control media (20 mM K^+) *DR5:GUS* expression was stronger (Figure 8d,f) than in Murashige–Skoog phytagel plates (Figure 7e,f). Consequently, some GUS activity was detected in young stellar cells adjacent to vascular initials in both wt and *trh1* roots grown on agarose plates (Figure 8d,f). Similar to the results shown in Figure 7(f), the *trh1* roots grown on agarose plates in 20 mM K^+ had strong *DR5:GUS* expression in stellar cells of DEZ (Figure 8f). This pattern of GUS staining was not observed in wt plants grown in control media. In 0.1 mM external K^+, however, the upper boundary of *DR5:GUS* expression in stele cell files of wt roots was extended basipetally almost to the DEZ (Figure 8c). In general, reduction in external [K^+] affected auxin distribution in the wt roots in a way similar to the *trh1* mutation, thus causing agravitropic growth.

Roots of the *trh1* plants grown in 0.1 mM K^+ were much thinner than roots grown in high K^+ and had shorter meristems (Figure 8e). In the *trh1* plants low external K^+ also affected *DR5:GUS* expression, which was high in stelar cell files spanning the entire length of the meristem and declined sharply at the transition to the elongation zone (Figure 8e).

The observed effects of potassium on *DR5:GUS* expression demonstrate that the distribution of auxin within the root tip is dependent on the availability of this cation. Similarity between potassium-deprived wt roots and potassium-sufficient *trh1* roots with regard to *DR5:GUS* expression and growth pattern (Figure 8b,c,f) suggests that TRH1-dependent auxin transport is regulated by external [K^+] or coupled to K^+ transport. The distortion of auxin profile caused by low [K^+] was, however, weaker than those caused by the *trh1* mutation (Figure 8c,d,f). Accordingly, the agravitropic phenotype of the wt plants grown in low [K^+] was not quite strong (Figure 8b) and root hair growth was not affected (Desbrosses *et al.*, 2003). Changes in auxin profile in *trh1* mutants grown in low [K^+] were also associated with changes in meristem organization (Figure 8e) and, probably, due to the latter, led to increases in VGI. This paradoxical phenomenon requires further exploration. Agravitropic growth of wt roots in low potassium (Figure 8b) might be an important adaptation reaction, which allows the primary root to avoid K^+-depleted patches in the soil. Probably, the TRH1 carrier plays a central role in this reaction because the response to external [K^+] is inversed in the *trh1* mutant (Figure 8b).

Discussion

TRH1 belongs to the *KT/KUP/HAK* potassium transporters consisting of 13 members in *Arabidopsis* (Maser *et al.*, 2001). The ability of some members of this family to transport K^+ has been demonstrated by various authors (Fu and Luan, 1998; Kim *et al.*, 1998; Quintero and Blatt, 1997; Rigas

et al., 2001; Santa-Maria *et al.*, 1997; Su *et al.*, 2002). However, the morphological phenotypes of plants homozygous for the *trh1* mutation cannot be rescued by elevated concentrations of external K^+ and, therefore, are not caused by decreased bulk K^+ supply to the plant (Desbrosses *et al.*, 2003; Rigas *et al.*, 2001). When K^+ was supplied in millimolar concentrations *trh1* plants displayed the mutant morphological phenotypes, but did not suffer from potassium starvation and accumulated biomass at the same rate as the wt plants (Desbrosses *et al.*, 2003). Mutation in another member of the *KT/KUP/HAK* family *SHY3* (*AtKT2*, *AtKUP2*) affects elongation of hypocotyl cells, although no difference in K^+ accumulation was detected between the wt plants and the mutant (Elumalai *et al.*, 2002). Interestingly, the *shy3-1* mutation did not affect the K^+ transport properties of the SHY3 protein, as assessed in *Escherichia coli* TK2463 strain carrying mutations in trkD (kup) and kdp K^+ uptake systems. This suggests that the *shy3-1* phenotype is due to the alteration of an unknown regulatory function of the protein rather than to the impairment in K^+ transport (Elumalai *et al.*, 2002).

Spatial separation between the site of major *TRH1* expression in the root cap (Figure 7a,b) and morphologically defective root hair cells in the *trh1* mutant (Figure 1b) suggests that the *TRH1* gene may act non-cell autonomously, i.e. this transporter is involved in signalling over the long distance rather than simply providing bulk potassium supply for cell elongation.

Expression of the *TRH1* gene in the root cap which is the site of gravity perception in the root (Audus, 1962; Blancaflor *et al.*, 1998; MacCleery and Kiss, 1999), is consistent with the proposed role for TRH1 in gravitropic response and by extension suggests a connection with long-distance auxin signalling. The rescue of morphological *trh1* phenotypes by exogenous auxin (Figures 1g,k and 3f–h) and experiments with radiolabelled IAA (Table 1, Figure 6) provide strong evidence for a role of TRH1 in the transport of auxin.

According to the current paradigm (Estelle, 1996), the bulk supply of auxin produced in shoots is delivered acropetally to the root cap through the stellar tissues. After lateral translocation across the periclinal plasma membrane in the columella cells, auxin is transported through the lateral root cap basipetally to the epidermal and cortical tissues in the elongation zone (Figure 9).

As a direct consequence of impaired auxin transport in the root cap of the *trh1* plants, auxin builds up in the stele, where it ectopically activates expression of the *DR5:GUS* construct (Figures 7f,h and 9). The accumulation of auxin above the root cap is probably accompanied by reduced basipetal auxin flow towards the epidermis and the cortex (Figure 9). The decrease in basipetal auxin flow (Figure 9) results in auxin levels sub-optimal for root hair growth and gravitropic response (Figure 1d,i). The net translocation of exogenous auxin (Table 1) was estimated as a rate of label accumulation in the tip when [^{3}H]IAA was supplied to the base. [^{3}H]IAA accumulated in the root tip in these experiments is spread between central cylinder and cortex/epidermis. The reduction in net auxin translocation in the *trh1* mutant (Table 1) supports the conclusion that auxin deprivation in the cortex and the epidermis is indeed more pronounced than the excess of auxin in the stele because of the defects in transportation in the root cap (Figure 7f,h and 9). In qRT-PCR experiments some residual *TRH1* expression was observed in the tissues above the apical zone (Figure 7c) and, therefore, we cannot rule out that cells outside the root cap might also contribute to the TRH1-dependent long-distance auxin translocation.

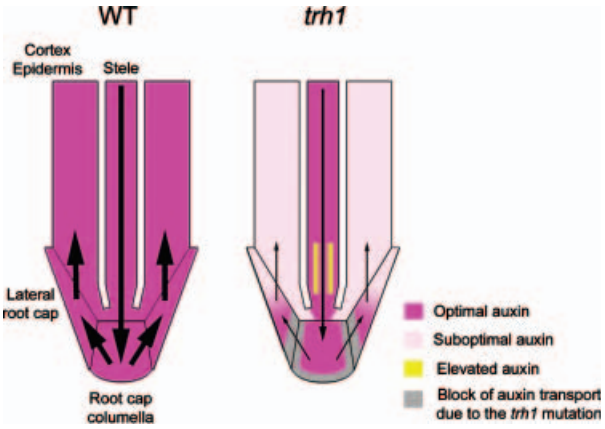

Figure 9. Auxin fluxes in the root tip of wild type (wt) and *trh1* plants. In wt plants auxin is delivered to the root cap acropetally through the central cylinder.
In the root cap the fluxes change direction basipetally and are diverted to the cortex/epidermis. TRH1 carrier, which is strongly expressed in the root cap, plays an important role in auxin translocation. Due to the *trh1* mutation auxin transport through the root cap is partially blocked. This block causes reduction in overall acropetal auxin transport and decreases in auxin concentration in the cortex/epidermis. Suboptimal auxin concentrations in cortical and epidermal tissues result in such defects as agravitropic root growth and impaired root hair elongation. Restricted flow of auxin through the root cap is also associated with auxin increases in some stellar cells upstream of the block. The contribution of these local increases to the total auxin concentration in the tip is, however, negligible compared with auxin deprivation in cortical and epidermal cells.

By definition, efflux transporters export auxin from the symplastic continuum into the apoplast and, thus, mediate not only directional auxin transport but also release of the phytohormone into a growth medium (Chen *et al.*, 1998). Data on accumulation and retention of labelled auxin (Table 1, Figure 6) enabled us to conclude that TRH1 facilitates phytohormone efflux similar to the putative auxin transporter AGR1/EIR1/AtPIN2, the mutation of which also affects gravitropic responses (Chen *et al.*, 1998; Luschnig *et al.*, 1998; Müller *et al.*, 1998a). Besides *agr1/eir1/Atpin2* (Chen *et al.*, 1998; Luschnig *et al.*, 1998), *trh1* roots exposed to exogenous auxin accumulated more phytohormone than roots of wt plants (Table 1). The reduced ability of the *trh1* root cells to expel excess exogenous auxin explains the

hypersensitivity to this phytohormone (Figure 3a–c,e) that was also observed in the auxin efflux transport mutants *agr1/eir1/Atpin2* (Chen *et al.*, 1998; Luschnig *et al.*, 1998; Müller *et al.*, 1998a). In contrast to *Atpin2*, the *trh1* roots displayed increased sensitivity to 2,4-D (Figure 3a,e) suggesting that this mutation affects different auxin transport pathways. In 2-NAA (Figure 3d) the differences in elongation of *trh1* and wt roots were less significant than in active auxins. On the basis of this observation we reason that the transport of 2-NAA is only partially dependent on TRH1 activity.

The agravitropic root behaviour of the *trh1* mutants can be phenocopied in wt plants by application of NPA (Figure 5b), a phytotropin which inhibits the auxin efflux (Delbarre *et al.*, 1996; Morgan and Söding, 1958; Sussman and Goldsmith, 1981). Although the gravitropic response of the *trh1* mutants was reduced in the presence of NPA, they were threefold less sensitive to the phytotropin than the wt plants. These data imply that the TRH1-dependent auxin transport is targeted by NPA in plants, but because this transport was not affected by the phytotropin in yeast (not shown), NPA might not directly interact with TRH1. Similarly, altered responses to NPA were observed in *eir1* mutants which are deficient in auxin efflux transport (Rashotte *et al.*, 2000). Basipetal auxin transport in the *eir1* plants was not only reduced in comparison with wt, but was also less sensitive to NPA (Rashotte *et al.*, 2000). As root elongation of *trh1* mutants and wt plants was equally affected by NPA (Figure 5a), we suggest that TRH1 is not involved in transport of the phytotropin.

Although molecular mechanisms of the TRH1-dependent auxin transport have not yet been identified, we speculate that this unexpected function of the potassium carrier might be explained by its ability to generate ionic and electric gradients across the plasma membrane that favour auxin efflux through other auxin transporters. If this holds true, the specific role of the TRH1 carrier in stimulation of auxin transport is, probably, due to its highly localized expression in the root cap (Figure 7). We cannot rule out that TRH1 may transport auxin directly, utilizing energy of coupled ion transport in a manner that has been described for K^+- and Na^+-dependent amino acid carriers (Androutsellis-Theotokis *et al.*, 2003; Castagna *et al.*, 1998) or through an uncoupled transport, which has been demonstrated in variety of transporters (Borre *et al.*, 2002; Chaudhry *et al.*, 2001; Ryan and Vandenberg, 2002). Multifunctional properties of TRK potassium transporters has been recently demonstrated in yeast (Kuroda *et al.*, 2004). These transporters also operate as channels mediating anion efflux from the cell. Similar mechanisms might be involved in the transport of the anionic form of auxin by the TRH1 potassium transporter, but at the moment no experimental data are available to support this suggestion.

Changes in auxin distribution and gravitropic behaviour caused by K^+ deprivation (Figure 8) indicate a link between K^+ and auxin transport. Some similarities between phenotypes of K^+-deprived wt plants and K^+-sufficient *trh1* plants (Figure 8) suggest that the TRH1 transporter serves as a molecular determinant of this link. Agravitropic root growth triggered by reduction in external potassium (Figure 8b) is, probably, an important component of mineral deficiency avoidance reaction, which enables roots to grow away from K^+-depleted patches. The altered K^+ dependence of VGI in the *trh1* mutant (Figure 8b) demonstrates that the TRH1 transporter is central for this reaction, probably regulating auxin fluxes in a K^+-dependent fashion. The localization of TRH1 to the very tip of the root is compatible with this function, but obviously more research is required to prove this hypothesis.

Experimental procedures

Plant material and growth conditions

Arabidopsis thaliana (Wassilewskija) seeds were surface-sterilized (Weigel and Glazebrook, 2002) and sown in 120 × 120 mm square Petri dishes (Greiner Bio-one, Frickenhausen, Germany) on 0.3 or 0.4% phytagel (Sigma, Gillingham, UK) supplemented with 1× Murashige–Skoog medium (Duchefa, Haarlem, The Netherlands), pH 5.6 and 30 mM sucrose (VWR, Lutterworth, UK). After 48 h stratification at 4°C, seedlings were grown on vertical plates for 2–6 DAG at 16/8 h 23/20°C day/night cycle. For the auxin transport assay, plants were cultured hydroponically in the Murashige–Skoog medium supplemented with 30 mM sucrose for 6 DAG as above. For the gravitropic assay (Marchant *et al.*, 1999), after stratification, seeds were germinated in light for 16 h, followed by 96 h growth in darkness. After the rotation of the plate by 90°, seedlings where grown in the dark. The position of the root tip was marked on the plate under the microscope immediately before rotation. Roots were grown in the dark for 7 h after rotation and gravitropic response was quantified as an angle between the tangents to the root growth trajectory immediately above and below the mark.

To study the effect of external K^+ on root morphology and *DR5:GUS* expression, plants were grown on Murashige–Skoog phytagel plates supplemented with 30 mM sucrose as above for 2 DAG. On the 2 DAG, plants were briefly washed in K^+-free liquid assay media transferred onto the plates containing assay media supplemented with different concentrations of KNO_3 and solidified with 7% purified Fluka agarose (Sigma). K^+-free assay media contained microelement mix (Somerville and Ogren, 1982), 30 mM sucrose and macronutrients: $NH_4H_2PO_4$–1.25 mM, NH_4NO_3 20 mM, $Ca(NO_3)_2$ 5 mM, NH_4Cl 3 mM, $MgSO_4$ 1.5 mM, $CaCl_2$ 1.5 mM, Ca-MES 2.5 mM and Fe(II)-EDTA 0.05 mM.

Morphometrics

In order to explore the soil efficiently, the main roots grow parallel to the vector of gravity with GSA equal to 0° (Digby and Firn, 1995; Ottenschlager *et al.*, 2003). This GSA enables plants to reach the deepest soil horizons in the most economical way at which the depth of apex penetration is equal to the root length

(RL). In agravitropic mutants this developmental programme is disrupted and the direction of the root growth deviates from vertical. In this case the depth of root apex penetration is equal to CH_Y, a projection of the base-to-tip chord *CH* on vertical axis (Figure 2a).

To characterize the pattern of main root development on 2D agar/air interface we used a morphometric parameter designated as VGI and defined as

$$VGI = \frac{CH_Y}{RL}$$

VGI, thus, is a quantitative measure of discrepancy between real and model root development. Because CH_Y is less than RL, the lowest and the highest values of the VGI are delimited by −1 and +1 respectively. −1 is attributed to the agravitropic phenotype with GSA = 180° and +1 corresponds to a model gravitropic downward growth (GSA = 0°). Diagravitropic growth perpendicular to the vector of gravity (GSA = 90°or 270°) is characterized by VGI = 0.

To analyse root geometry, plates with seedlings were either scanned with ScanJet 6300C scanner (Hewlett Packard, Boise, ID, USA) or photographed with DP-10 (Olympus, Tokyo, Japan) digital camera attached to SZX9 (Olympus) stereomicroscope. The obtained images were analysed with ImageJ 1.20 (http://rsb.info.nih.gov/ij) and SigmaPlot 7.0 (SPSS Science, Birmingham, UK) software.

Half inhibition (IC_{50}) and effective mid-point concentrations (EC_{50}) in the dose–response curves (Figures 3 and 5) were determined with use of Marquardt (1963) algorithm through fitting Hill equation to the experimental data (Grabov and Blatt, 1997).

Measurement of auxin fluxes in roots

Apical root segments (15–20 mm) isolated from 6 DAG plants were incubated at room temperature in a liquid growth medium supplemented with 74 nM [^{3}H]IAA (Amersham Pharmacia Biotech, Little Chalfont, UK). To measure auxin accumulation, after 2 h incubation 10 segments were washed five times with 100 μM unlabelled IAA solution, blotted with filter paper and weighed. After overnight solubilization in 10% SDS, label accumulation was measured by liquid scintillation counting using Rackbeta 1211 (LKB-Wallac, Turku, Finland). The diffusion-based accumulation of [^{3}H]IAA was measured in the presence of 100 μM unlabelled IAA and was subtracted from the total accumulation (Marchant *et al.*, 1999). To measure the rate of auxin efflux, after incubation in [^{3}H]IAA-containing medium for 15 min, root segments were washed in the same medium but without the addition of auxin. After 3 h of wash, radioactivity of the segments was measured as described above.

The acropetal transport of auxin was measured in a chamber containing two compartments bounded by walls made of hydrophobic plastic and separated by 2 mm gap. Defoliated plant segments were placed in the chamber in such a way that they bridged the two compartments. The compartment with hypocotyls was filled with the nutrient media containing labelled IAA, while the root tips in another compartment were bathed in auxin-free medium. The water-repelling properties of the hydrophobic plastic and the air gap prevented direct solution exchange between the compartments and, therefore, radioactivity detected in the root tips could only originate from the polar acropetal auxin translocation. The segments were incubated in the chamber for 60 min. After incubation, the apical parts were cut from the rest of the segments, washed and analysed using liquid scintillation counting as described above.

Yeast strains and [^{3}H]IAA transport experiments

Saccharomyces cerevisiae strain M398 expressing, either *TRH1* gene or empty pVT100U vector (Rigas *et al.*, 2001), were grown in YEDP media (BiO1001, Carlsbad, NM, USA) at 30°C for 2 days. After harvesting by centrifugation at 1258 ***g*** for 5 min, cells were re-suspended in the buffer containing 10 mM MES (pH = 5.6), 2% glucose, 1 mM $CaCl_2$ and 10 mM $(NH_4)_2SO_4$ supplemented with 74 nM [^{3}H]IAA. After 15 min incubation, cells (1.5×10^6 per sample) were washed four times on GF/C filters (PAL, Ann Arbor, MI, USA) using ice-cold 100 μM unlabelled IAA solution and solubilized overnight in 10% SDS. The label accumulation was measured by liquid scintillation counting. To measure auxin efflux, cells were pre-incubated for 5 min in the buffer containing [^{3}H]IAA solution, harvested by centrifugation at 1258 ***g*** for 1 min, and re-suspended in an auxin-free buffer. After washing in the buffer, the remaining radioactivity was measured as above.

Pro_{TRH1}:GUS and DR5:GUS expression

An approximately 2000 bp region of the *TRH1* gene regulatory sequences, which contains the region from position −2013 to −14 upstream of the translation initiation (ATG), was amplified from *Arabidopsis* genomic DNA. The oligonucleotides used for the polymerase chain reaction (PCR) were 5′-AAGCTTGTCGACAGGCTGATATCTGGAGTGCTGGTGTGA-3′ and 5′-GAATTCGGATCCGCGAGTAAGATGCGGCGTAGCTTGG-3′. The underlined hexanucleotide sequences correspond to the *Sal*I and *Bam*HI restriction sites, respectively, which were introduced to facilitate cloning. The PCR product was directionally cloned into the *Sal*I/*Bam*HI sites of the pBI101.1 binary vector (Clontech, Palo Alto, CA, USA), as a promoter for the *GUS* reporter gene cassette. The binary vector construct was introduced into the *Agrobacterium tumefaciens* strain C58C1::pGV3101 by electroporation. *Arabidopsis thaliana* plants, ecotype *Columbia*, were transformed by the *A. tumefaciens* infiltration method (Weigel and Glazebrook, 2002). Transgenic plants were selected on MS growth medium, which contained 50 mg l^{-1} kanamycin.

The *DR5:GUS* construct was subcloned in SLJ755I6 binary vector (http://www.sainsbury-laboratory.ac.uk/jonathan-jones/plasmid-list/plasmid.htm) which was used to transform *A. tumefaciens* (LBA 4404) cells by electroporation. Wild-type and *trh1* plants were transformed with the construct using the floral dip method (Weigel and Glazebrook, 2002). Transgenic plants were selected in soil by spraying with 300 μM DL-phospinotricin (Duchefa).

To localize β-glucuronidase activity, roots of 4–5 DAG transgenic plants were incubated overnight at 37°C in 0.1 M phosphate buffer pH 7 containing 1 mM X-Gluc, 0.1% Triton X-100 and 4 mM potassium ferricyanide. Stained tissues were cleared as described by Malamy and Benfey (1997) and mounted in 50% glycerol on glass slides. For the preparation of histological sections, GUS-stained roots were dehydrated in ethanol and embedded in Technovit 7100 resin (Heraeus-Kuzler, Wehrheim, Germany). Sections (4 μm) were stained in 0.05% ruthenium red and mounted in Histomount (National Diagnostics, Hessle, UK).

Preparations were viewed with IX70 (Olympus) microscope using differential interference contrast optics. Images were captured with DP-10 (Olympus) digital camera.

Plants for qRT-PCR analysis were grown on vertical MS phytagel plates as above. Plants (5 DAG) were transferred from the plates to RNA*later* solution (Ambion, Huntingdon, UK). Roots of wt and *trh1* plants submerged in RNA*later* were dissected under a stereomicroscope. Using vacuum tweezers (Vacuseed; Polaris Instruments, Diddington, UK) 0.6 mm root apices and 10 mm decapitated root

segments were transferred to the wells of 96-well titration plates where they were stored in RNA*later* solution before purification. RNA was purified using RNEasy Plant kit (Qiagen, Crawley, UK) and treated with RNase-free DNase (Qiagen). Total RNA in the samples (three replicates, 35 to 48 plants in each replicate) was quantified using fluorescent indicator Ribogreen (Molecular Probes, Leiden, The Netherlands) and RNA standards provided by the manufacturer. RNA samples were reverse transcribed with Omniscript (Qiagen) and Oligo$(dT)_{15}$ primers (Promega, Southampton, UK). Synthesized cDNA was further purified using QIAquick PCR purification columns (Qiagen) and cycled with QuantiTect SYBR Green PCR mix (Qiagen) in Rotor-Gene 3000 (Corbett Research, Sydney, Australia) using primers 5′-GAGCATCGCCGAGTTTATCCAG-3′ and 5′-GCTCCGGCAATTCTTCCTCAA-3′. Calibration curve was obtained through cycling plasmid DNA containing full-length *TRH1* cDNA. Concentrations of TRH1 transcript in the samples were calculated using this calibration curve and normalized to total RNA in each sample.

Acknowledgements

The authors thank Jane Murfett and Tom Guilfoyle for the DR5:GUS construct, Jonathan Jones for the SLJ755I6 binary vector, Paul Linstead for SEM and Richard Gaber for the M398 yeast strain and the shuttle vector pVT100U. The pGPTV-HTP binary vector was kindly provided by Jeff Schell. This research was supported by the UK Biotechnology and Biological Sciences Research Council (AG and LD) and Royal Society (AG).

References

Aberg, B. (1957) Auxin relations in roots. *Annu. Rev. Plant Physiol.* **8**, 153–180.

Ahn, S.J., Shin, R. and Schachtman, D.P. (2004) Expression of KT/KUP genes in *Arabidopsis* and the role of root hairs in K^+ uptake. *Plant Physiol.* **134**, 1135–1145.

Androutsellis-Theotokis, A., Goldberg, N.R., Ueda, K., Beppu, T., Beckman, M.L., Das, S., Javitch, J.A. and Rudnick, G. (2003) Characterization of a functional bacterial homologue of sodium-dependent neurotransmitter transporters. *J. Biol. Chem.* **278**, 12703–12709.

Audus, L.J. (1962) The mechanisms of the perception of gravity by plants. In *Biological Receptor Mechanisms* (Society for Experimental Biology, Symposium 16). Cambridge: Cambridge University Press, pp. 197–226.

Baker, D.A. (2003) Long-distance vascular transport of endogenous hormones in plants and their role in source:sink regulation. *Israel J. Plant Sci.* **48**, 199–203.

Bhalerao, R.P., Eklof, J., Ljung, K., Marchant, A., Bennett, M. and Sandberg, G. (2002) Shoot-derived auxin is essential for early lateral root emergence in *Arabidopsis* seedlings. *Plant J.* **29**, 325–332.

Blancaflor, E.B., Fasano, J.M. and Gilroy, S. (1998) Mapping the functional roles of cap cells in the response of *Arabidopsis* primary roots to gravity. *Plant Physiol.* **116**, 213–222.

Borre, L., Kavanaugh, M.P. and Kanner, B.I. (2002) Dynamic equilibrium between coupled and uncoupled modes of a neuronal glutamate transporter. *J. Biol. Chem.* **277**, 13501–13507.

Castagna, M., Shayakul, C., Trotti, D., Sacchi, V.F., Harvey, W.R. and Hediger, M.A. (1998) Cloning and characterization of a potassium-coupled amino acid transporter. *Proc. Natl Acad. Sci. USA*, **95**, 5395–5400.

Chaudhry, F.A., Krizaj, D., Larsson, P., Reimer, R.J., Wreden, C., Storm-Mathisen, J., Copenhagen, D., Kavanaugh, M. and Edwards, R.H. (2001) Coupled and uncoupled proton movement by amino acid transport system N. *EMBO J.* **20**, 7041–7051.

Chen, R.J., Hilson, P., Sedbrook, J., Rosen, E., Caspar, T. and Masson, P.H. (1998) The *Arabidopsis thaliana AGRAVITROPIC 1* gene encodes a component of the polar-auxin-transport efflux carrier. *Proc. Natl Acad. Sci. USA*, **95**, 15112–15117.

Cholodny, N.G. (1924) Über die hormonale wirkung der Organspitze bei der geotropischen Krümmung. *Ber. Deutsch. Bot. Ges.* **42**, 356–362.

Collett, C.E., Harberd, N.P. and Leyser, O. (2000) Hormonal interactions in the control of *Arabidopsis* hypocotyl elongation. *Plant Physiol.* **124**, 553–561.

Delbarre, A., Muller, P., Imhoff, V. and Guern, J. (1996) Comparison of mechanisms controlling uptake and accumulation of 2,4-dichlorophenoxy acetic acid, naphthalene-1-acetic acid, and indole-3-acetic acid in suspension-cultured tobacco cells. *Planta*, **198**, 532–541.

Desbrosses, G., Josefsson, C., Rigas, S., Hatzopoulos, P. and Dolan, L. (2003) *AKT1* and *TRH1* are required during root hair elongation in *Arabidopsis*. *J. Exp. Bot.* **54**, 781–788.

Digby, J. and Firn, R.D. (1995) The gravitropic set-point angle (GSA): the identification of an important developmentally controlled variable governing plant architecture. *Plant Cell Environ.* **18**, 1434–1440.

Dolan, L. (1998) Pointing roots in the right direction: the role of auxin transport in response to gravity. *Genes Dev.* **12**, 2091–2095.

Elumalai, R.P., Nagpal, P. and Reed, J.W. (2002) A mutation in the *Arabidopsis KT2/KUP2* potassium transporter gene affects shoot cell expansion. *Plant Cell*, **14**, 119–131.

Estelle, M. (1996) Plant tropisms: the ins and outs of auxin. *Curr. Biol.* **6**, 1589–1591.

Firn, R.D., Wagstaff, C. and Digby, J. (2000) The use of mutants to probe models of gravitropism. *J. Exp. Bot.* **51**, 1323–1340.

Friml, J. (2003) Auxin transport – shaping the plant. *Curr. Opin. Plant Biol.* **6**, 7–12.

Friml, J., Benkova, E., Blilou, I. *et al.* (2002a) AtPIN4 mediates sink-driven auxin gradients and root patterning in *Arabidopsis*. *Cell*, **108**, 661–673.

Friml, J., Wisniewska, J., Benkova, E., Mendgen, K. and Palme, K. (2002b) Lateral relocation of auxin efflux regulator PIN3 mediates tropism in *Arabidopsis*. *Nature*, **415**, 806–809.

Fu, H.H. and Luan, S. (1998) AtKUP1: a dual-affinity K^+ transporter from *Arabidopsis*. *Plant Cell*, **10**, 63–73.

Fujita, H. and Syono, K. (1996) Genetic analysis of the effects of polar auxin transport inhibitors on root growth in *Arabidopsis thaliana*. *Plant Cell Physiol.* **37**, 1094–1101.

Fukaki, H., Tameda, S., Masuda, H. and Tasaka, M. (2002) Lateral root formation is blocked by a gain-of-function mutation in the SOLITARY-ROOT/IAA14 gene of *Arabidopsis*. *Plant J.* **29**, 153–168.

Gaedeke, N., Klein, M., Kolukisaoglu, U. *et al.* (2001) The *Arabidopsis thaliana* ABC transporter *At*MRP5 controls root development and stomata movement. *EMBO J.* **20**, 1875–1887.

Grabov, A. and Blatt, M.R. (1997) Parallel control of the inward-rectifier K^+ channel by cytosolic free Ca^{2+} and pH in *Vicia* guard cells. *Planta*, **201**, 84–95.

Hobbie, L. and Estelle, M. (1995) The *axr4* auxin-resistant mutants of *Arabidopsis thaliana* define a gene important for root gravitropism and lateral root initiation. *Plant J.* **7**, 211–220.

Katekar, G.F. and Geissler, A.E. (1980) Auxin transport inhibitors. 4. Evidence of a common mode of action for a proposed class of auxin transport inhibitors – the phytotropins. *Plant Physiol.* **66**, 1190–1195.

Keitt, G.W. and Baker, R.A. (1966) Auxin activity of substituted benzoic acids and their effect on polar auxin transport. *Plant Physiol.* **41**, 1561–1569.

Kim, E.J., Kwak, J.M., Uozumi, N. and Schroeder, J.I. (1998) *AtKUP1*: an *Arabidopsis* gene encoding high-affinity potassium transport activity. *Plant Cell*, **10**, 51–62.

Kuroda, T., Bihler, H., Bashi, E., Slayman, C.L. and Rivetta, A. (2004) Chloride channel function in the yeast TRK-potassium transporters. *J. Membr. Biol.* **198**, 177–192.

Lane, R.H. (1936) The inhibition of roots by growth hormone. *Am. J. Bot.* **23**, 532–535.

Leyser, H.M.O., Pickett, F.B., Dharmasiri, S. and Estelle, M. (1996) Mutations in the AXR3 gene of *Arabidopsis* result in altered auxin response including ectopic expression from the SAUR-AC1 promoter. *Plant J.* **10**, 403–413.

Luschnig, C., Gaxiola, R.A., Grisafi, P. and Fink, G.R. (1998) EIR1, a root-specific protein involved in auxin transport, is required for gravitropism in *Arabidopsis thaliana*. *Genes Dev.* **12**, 2175–2187.

MacCleery, S.A. and Kiss, J.Z. (1999) Plastid sedimentation kinetics in roots of wild-type and starch-deficient mutants of *Arabidopsis*. *Plant Physiol.* **120**, 183–192.

Malamy, J.E. and Benfey, P.N. (1997) Organization and cell differentiation in lateral roots of *Arabidopsis thaliana*. *Development*, **124**, 33–44.

Marchant, A., Kargul, J., May, S.T., Muller, P., Delbarre, A., Perrot-Rechenmann, C. and Bennett, M.J. (1999) AUX1 regulates root gravitropism in *Arabidopsis* by facilitating auxin uptake within root apical tissues. *EMBO J.* **18**, 2066–2073.

Marquardt, D.W. (1963) An algorithm for least squares estimation of parameters. *J. Soc. Ind. Appl. Math.* **11**, 431–441.

Maser, P., Thomine, S., Schroeder, J.I. *et al.* (2001) Phylogenetic relationships within cation transporter families of *Arabidopsis*. *Plant Physiol.* **126**, 1646–1667.

Masucci, J.D. and Schiefelbein, J.W. (1996) Hormones act downstream of TTG and GL2 to promote root hair outgrowth during epidermis development in the *Arabidopsis* root. *Plant Cell*, **8**, 1505–1517.

Meesters, A. (1936) The influence of hetero-auxin on the growth of root hairs and roots of *Agrostemma Githago* L. *Proc. Kon. Akad. Wetensch. Amsterdam*, **39**, 91–97.

Morgan, D.G. and Söding, H. (1958) Über die Wirkungsweise von Phthalsäuremono-α-Naphthylamide (PNA) auf das Wachstum der Haferkoleoptile. *Planta*, **52**, 235–249.

Mullen, J.L., Ishikawa, H. and Evans, M.L. (1998) Analysis of changes in relative elemental growth rate patterns in the elongation zone of *Arabidopsis* roots upon gravistimulation. *Planta*, **206**, 598–603.

Müller, A., Guan, C.H., Galweiler, L., Tanzler, P., Huijser, P., Marchant, A., Parry, G., Bennett, M., Wisman, E. and Palme, K. (1998a) *AtPIN2* defines a locus of *Arabidopsis* for root gravitropism control. *EMBO J.* **17**, 6903–6911.

Müller, A., Hillebrand, H. and Weiler, E.W. (1998b) Indole-3-acetic acid is synthesized from L-tryptophan in roots of *Arabidopsis thaliana*. *Planta*, **206**, 362–369.

Nagpal, P., Walker, L.M., Young, J.C., Sonawala, A., Timpte, C., Estelle, M. and Reed, J.W. (2000) AXR2 encodes a member of the Aux/IAA protein family. *Plant Physiol.* **123**, 563–573.

Noh, B., Murphy, A.S. and Spalding, E.P. (2001) *Multidrug resistance*-like genes of *Arabidopsis* required for auxin transport and auxin-mediated development. *Plant Cell*, **13**, 2441–2454.

Ottenschlager, I., Wolff, P., Wolverton, C., Bhalerao, R.P., Sandberg, G., Ishikawa, H., Evans, M. and Palme, K. (2003) Gravity-regulated differential auxin transport from columella to lateral root cap cells. *Proc. Natl Acad. Sci. USA*, **100**, 2987–2991.

Quintero, F.J. and Blatt, M.R. (1997) A new family of K^+ transporters from *Arabidopsis* that are conserved across phyla. *FEBS Lett.* **415**, 206–211.

Rahman, A., Hosokawa, S., Oono, Y., Amakawa, T., Goto, N. and Tsurumi, S. (2002) Auxin and ethylene response interactions during *Arabidopsis* root hair development dissected by auxin influx modulators. *Plant Physiol.* **130**, 1908–1917.

Rashotte, A.M., Brady, S.R., Reed, R.C., Ante, S.J. and Muday, G.K. (2000) Basipetal auxin transport is required for gravitropism in roots of *Arabidopsis*. *Plant Physiol.* **122**, 481–490.

Rigas, S., Desbrosses, G., Haralampidis, K., Vicente-Agullo, F., Feldmann, K.A., Grabov, A., Dolan, L. and Hatzopoulos, P. (2001) *TRH1* encodes a potassium transporter required for tip growth in *Arabidopsis* root hairs. *Plant Cell*, **13**, 139–151.

Rubio, F., Santa-Maria, G.E. and Rodriguez-Navarro, A. (2000) Cloning of *Arabidopsis* and barley cDNAs encoding HAK potassium transporters in root and shoot cells. *Physiol. Plant.* **109**, 34–43.

Ryan, R.M. and Vandenberg, R.J. (2002) Distinct conformational states mediate the transport and anion channel properties of the glutamate transporter EAAT-1. *J. Biol. Chem.* **277**, 13494–13500.

Sabatini, S., Beis, D., Wolkenfelt, H. *et al.* (1999) An auxin-dependent distal organizer of pattern and polarity in the *Arabidopsis* root. *Cell*, **99**, 463–472.

Santa-Maria, G.E., Rubio, F., Dubcovsky, J. and Rodriguez-Navarro, A. (1997) The *HAK1* gene of barley is a member of a large gene family and encodes a high-affinity potassium transporter. *Plant Cell*, **9**, 2281–2289.

Schiefelbein, J.W., Masucci, J.D. and Wang, H.Y. (1997) Building a root: the control of patterning and morphogenesis during root development. *Plant Cell*, **9**, 1089–1098.

Simmons, C., Migliaccio, F., Masson, P., Caspar, T. and Soll, D. (1995) A novel root gravitropism mutant of *Arabidopsis thaliana* exhibiting altered auxin physiology. *Physiol. Plant.* **93**, 790–798.

Somerville, C.R. and Ogren, W.L. (1982) Isolation of photorespiration mutants in *Arabidopsis thaliana*. In *Methods in Chloroplast Biology* (Edelman, M., Hallick, R.B. and Chua, N.H., eds). Amsterdam: Elsevier Biomedical Press, pp. 129–138.

Su, H., Golldack, D., Zhao, C.S. and Bohnert, H.J. (2002) The expression of HAK-type K^+ transporters is regulated in response to salinity stress in common ice plant. *Plant Physiol.* **129**, 1482–1493.

Sussman, M.R. and Goldsmith, M.H.M. (1981) Auxin uptake and action of N-1-naphthylphthalamic acid in corn coleoptiles. *Planta*, **150**, 15–25.

Swarup, R., Friml, J., Marchant, A., Ljung, K., Sandberg, G., Palme, K. and Bennett, M. (2001) Localization of the auxin permease AUX1 suggests two functionally distinct hormone transport pathways operate in the *Arabidopsis* root apex. *Genes Dev.* **15**, 2648–2653.

Thimann, K.V. (1936) Auxin and the growth of roots. *Am. J. Bot.* **23**, 561–569.

Torrey, J.G. (1950) The induction of lateral roots by indoleacetic acid and root decapitation. *Am. J. Bot.* **4**, 257–264.

Ulmasov, T., Murfett, J., Hagen, G. and Guilfoyle, T.J. (1997) Aux/IAA proteins repress expression of reporter genes containing natural and highly active synthetic auxin response elements. *Plant Cell*, **9**, 1963–1971.

Weigel, D. and Glazebrook, J. (2002) *Arabidopsis*. A Laboratory Manual. New York: CSHL Press.

Went, F.W. and Thimann, K.V. (1937) *Phytohormones*. New York: Macmillan.